BMBF Verbundprojekt

Report on DKRZ Resources 2020

PalMod – Paleo Modeling Initiative Phase II:

From the Last Interglacial to the Anthropocene –
Modelling a Complete Glacial Cycle

Principal Investigators: Mojib Latif[1],
Tatiana Ilyina[2],
Michael Schulz[3]

(1) GEOMAR, Kiel (to whom correspondence should be sent)
(2) MPI-M, Hamburg
(3) MARUM, Bremen

Executive Summary

The report summarizes the individual reports of the projects associated to the consortium project **PalMod II** and covers the time period from 2020-01-01 to 2020-12-31. The numbers shown in the following reflect the status 15. October 2020 unless stated otherwise.

Table of Contents

Preface

We want to highlight the reasons, why we were not able to use the computing time granted by WLA for 2020 to an appropriate amount.

The project PalMod I officially ended in September 2019, but nearly half of the projects received “kostenneutrale Verlängerung” (cost neutral project extension) for up to 18 months beyond end of 2020. Thus, during the year we had projects and groups working in PalMod I and projects and groups working in PalMod II.

This transfer went along with a changing in the staff, scientists were leaving and positions had to be filled - what became a problematic task during 2020. While finding suitable candidates was challenging but possible, it became difficult for the appointed scientists to enter Germany. As a consequence, the work packages could not fully start to work towards the PalMod II project goals and the introduction of the new colleagues is still ongoing.

This influences the setup and execution of the experiments planned for 2020. The models used here will be first-of-its-kinds with respect to the complexity. It was the target for 2020 to perform the first simulations with the fully coupled model system at DKRZ resources, but due to the shortage of staff the porting of the models from local resources to DKRZ had to be postponed.

All this together led to an adaption of the project plan and we had to postpone some of the central experiments and ensemble simulations planned for 2020 to 2021. The adaption of the work plan is communicated to and accepted by the Projektträger DLR and we are confident, that our project plan for 2021 will be more realistic.

1. Project 989

Project title: Long transient simulations of the last glacial cycle (last 130,000 years) and the development of lithosphere and ice sheet models
Project leader: Prof. Dr. Gerrit Lohmann, Dr. Gregor Knorr, Dr. Volker Klemann (GFZ), Dr. Uwe Mikolajewicz (MPI-Met)
Allocation period: 01.01.2020 – 15.10.2020

1.1 Report on resources used in 2020

The GFZ (PalMod-2 WP1.4-TP1) utilized VILMA to reconstruct the glacial-isostatic adjustment (GIA) as the solid-Earth component in PalMod. We extended our model ensemble to investigate the effect of 3D Earth structure variations on variability of relative sea-level (RSL) during the last glacial cycle. The ensemble of 3D Earth structures is derived from seismic tomography models and geodynamic constraints and differ in lithospheric thickness and lateral and radial viscosity distribution. Figure 1a shows the variations in the Earth structure ensemble for the 18 ensemble members that differ in conversion from seismic velocity to temperature variations (variations within classes) and radial "background" viscosity profiles (variations between classes). Figure 1b visualizes the global distribution of lateral variations for the ensemble mean for the asthenosphere viscosity. Using VILMA, we predicted the RSL applying the Earth structure ensemble members and different ice histories. Figure 1c shows the RSL predictions at 14 ka BP for the ICE-5G and Figure 1d for the ICE-6G history. The results show significant RSL variability of >100 m (ice center), tens of meter (near-field/forebulge) and <10 m (far-field).

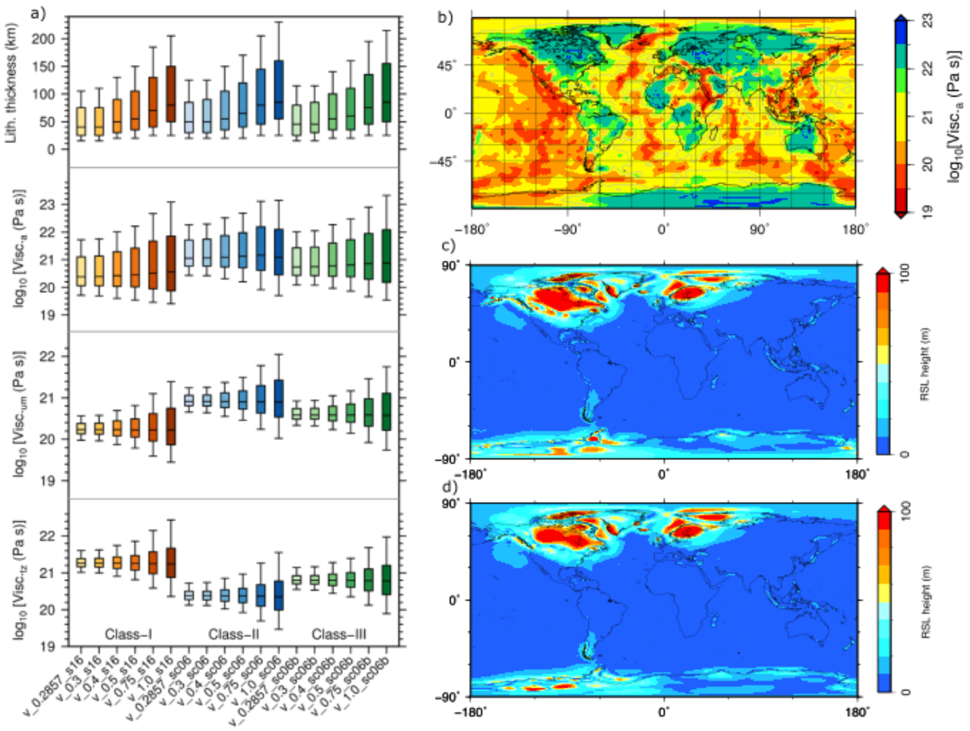

Figure 1: (a) Median and percentiles (5th, 25th, 75th and 90th) for the lithospheric thickness and for the average viscosity of the asthenosphere (a), upper mantle (um) and transition zone (tz) for 18 3D viscosity structures for three classes of viscosity contrast in the transition zone. (b) Ensemble mean for 18 3D viscosity structures shown as average of viscosity for the asthenosphere. (c, d) Ensemble range for the RSL prediction at 14 ka BP realized with the 3D model ensemble calculated with ice history (c) ICE-5G and (d) ICE-6G. (Bagge et al. 2020)

At MPI-Met, we added an interactive iceberg module to our fully coupled MPI-ESM-CR-PISM-VILMA model setup. We optimized the model parameters of the coupled model system for the last deglaciation using asynchronously coupled simulations, which resulted in physically plausible deglaciation scenarios of the northern hemisphere. We also performed deglaciation simulations starting from 26 kyrs BP and 18 kyrs BP, using synchronous coupling with parameter settings from the asynchronous simulations. Some of the runs are still ongoing. The coupled model reproduces abrupt climate events. The phasing differs in many simulations indicating the stochastic contribution to the timing of these events (Figure 2).

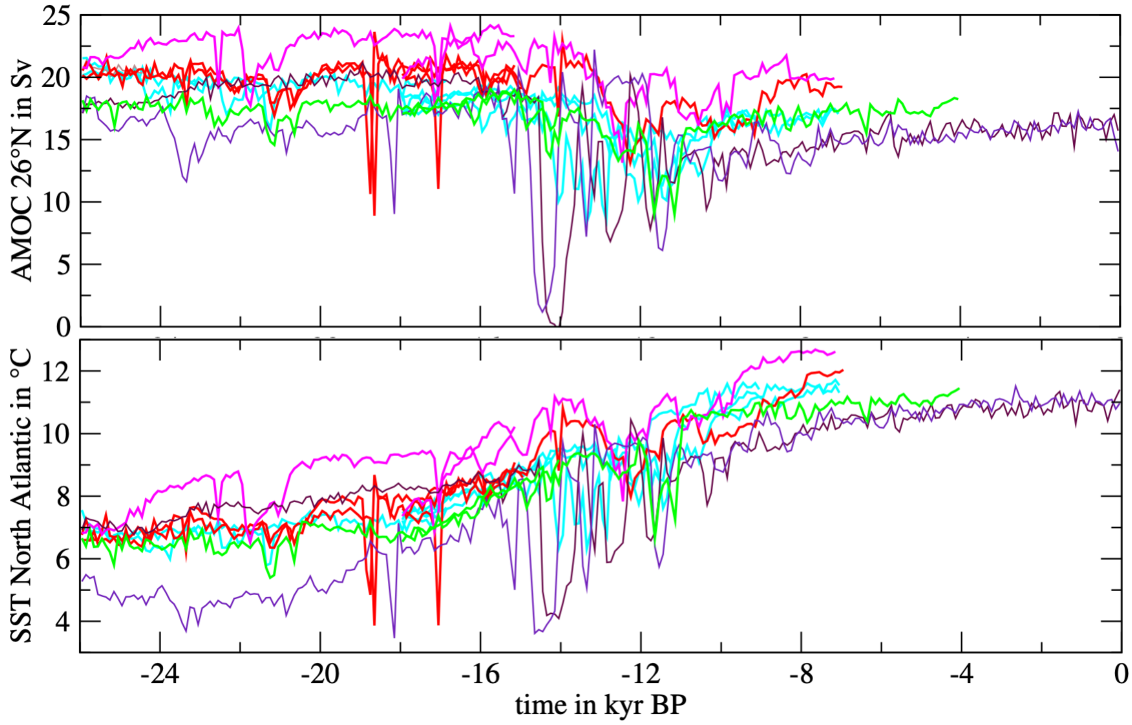

Figure 2: Timeseries of the Atlantic Meridional Overturning Circulation at 26°N (top) and the North Atlantic sea-surface temperature (bottom) from transient simulations of the last deglaciation. Brown and purple colors indicate simulations with prescribed ice sheets from the Ice6G and Glac1D ice-sheet reconstructions, respectively. All other lines indicate synchronously coupled simulations with the fully coupled MPI-Met climate ice-sheet model, differing in terms of tuning and initial conditions. The colours indicate different model versions, the latest ones in red and magenta. The coupled model simulates abrupt climate events as well as prominent past climate changes, similar to the Bølling-Allerød warm period (around 14 kyr BP) and the Younger Dryas (about 12.5 kyr BP).

In an ensemble of deglaciation simulations using MPI-ESM-CR with prescribed ice sheets and different atmosphere and ocean tuning, we investigated the effect of different ice sheet reconstructions on the climate response. These simulations reveal significant differences in the climate response, especially during the early part of the last deglaciation when northern ice sheets are still extensive. This underlines that uncertainties in the reconstructions are crucial for the climate response in our model.

We also have started accelerated simulations with MPI-ESM-CR-PISM-VILMA for the glacial inception (WP1.3), but these simulations have been delayed due to parental leave of the responsible post doc and an, in general, hampered progress due to the global pandemic and the resulting working conditions (e.g. interpersonal communication). Furthermore, the planned simulations of WP1.2 could not be performed due to a delay in hiring a new postdoc because of the pandemic (the position is expected to be filled in December)

The AWI has improved the modelling toolbox in 2020 to meet the needs that arise in the framework of PalMod2. Recent developments have significantly improved the computational efficiency and scalability of unstructured network approaches on high-performance computer systems (Danilov et al., 2017; Koldunov et al., 2019). Given the current highperformance computing power and the efficient and parallelized model code of FESOM, it is now possible to use our innovative model framework for transient simulations (Barbi et al., 2020; Lohmann et al., 2020; Gierz et al., 2020; Ackermann et al., 2020). We expect almost exclusively an atmospheric resolution T63.

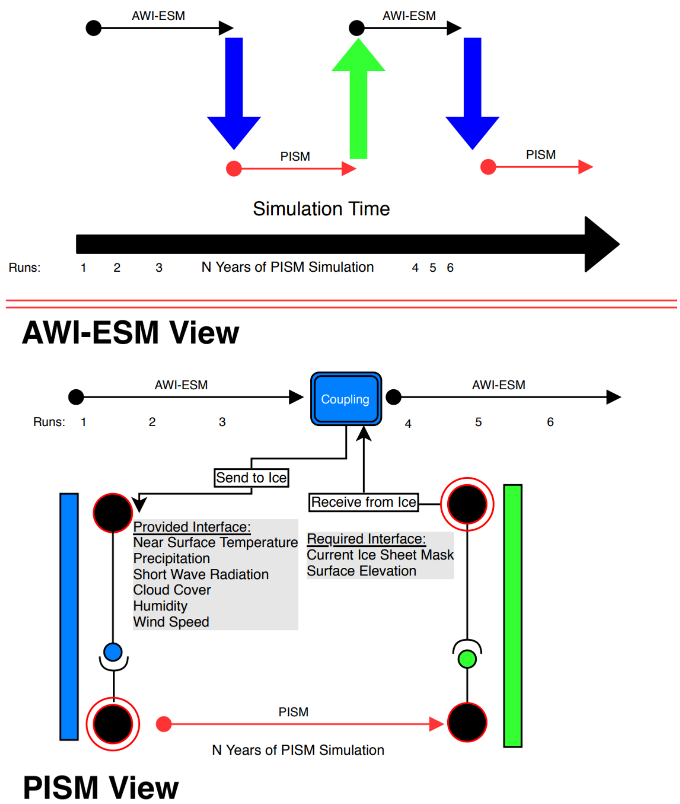

Figure 3: Schematic of AWI-ESM-1-2. The upper panel shows the two models running iteratively, whereas the bottom panel depicts the SCOPE coupling procedures (Gierz et al., 2020).

Furthermore, we have been working on a bi-hemispheric PISM set-up to enable simultaneous simulations of the Northern and Southern Hemisphere ice sheets. Both ice sheets are situated in one PISM domain. A deep artificial trench divides both hemispheres and prevents ice sheet growth or mass and heat fluxes from one hemisphere into the other. A first test run with a resolution of 20 km has been done for the pre-industrial control state (Figure 4).

Together with PalMod CC.1, the AWI invested a considerable amount of time into improving the atmosphere component of AWI-ESM2.1 and AWI-ESM2.2. In particular, a major effort was replacing the conventional radiation code in ECHAM6, with the goal of allowing the simulation throughput that is necessary to conduct long transient simulations that are a precondition for accomplishing PalMod2's scientific goals. Implementation, testing, and debugging of the ECHAM6 version with concurrent radiation has been significantly more difficult and time consuming than expected. Yet, this work is now finally bearing fruit. An additional task has been the finalization and documentation of the AWI-ESM2.2 (Gierz et al., 2020), the ice-sheet enabled version of the AWI-ESM2. The model system is based on the SCOPE coupler (Figure 3) that serves as the interface between AWI-ESM2 and the cryosphere model components. This work included reimplementation of the coupling of PISM to AWI-ESM2 towards sustainable use of the coupled model setup in the framework of the modular earth system modelling framework – that explicitly includes enabling its continued reuse beyond PalMod2. Aforementioned work has been more difficult than expected. Overall, switching to the new coupled model system AWI-ESM2.2 in the framework of PalMod2, technical difficulties involved in this process, together with reorganizing the work among new colleagues within PalMod2, and last but not least challenges in updating our work procedures in the context of CoVid-19, has unfortunately lead to a significant loss of computational time in 2020.

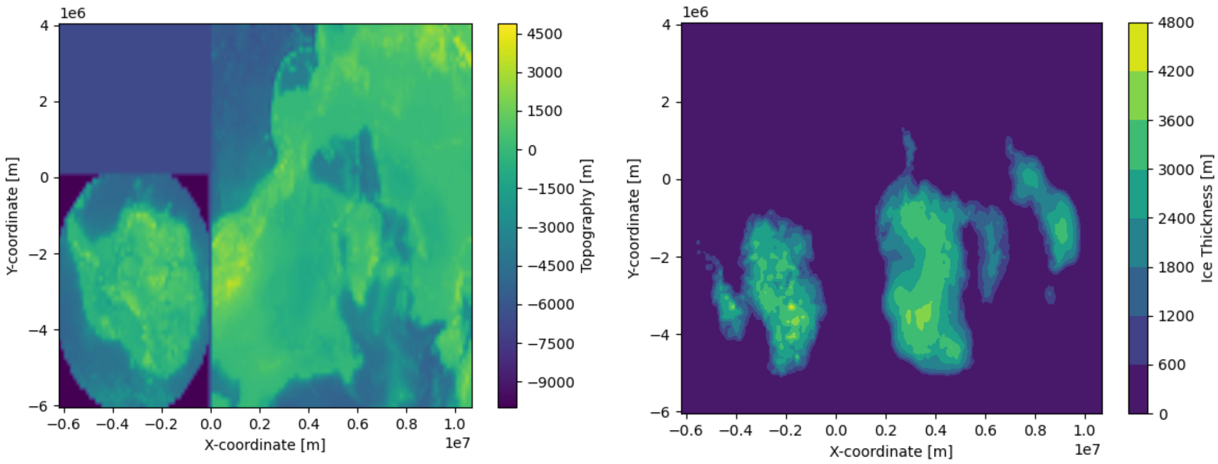

Figure 4: Topography and simulated ice thickness in the bihemispheric ice-sheet setup of PISM for pre-industrial climate forcing and geography. Antarctica is shown to the left in each of the plot panels, ice sheet regions of the Northern Hemisphere are shown to the right

Our scientific work within PalMod at AWI during the year 2020 has included various aspects. The performance of the climate component of the AWI-ESM2.2 has been evaluated in the context of other PMIP models for the Last Glacial Maximum (Kageyama et al., 2020) and the Last Interglacial (Otto-Bliesner et al., 2020). The surface mass balance scheme dEBM employed in AWI-ESM2.2 has been validated in the framework of the GrSMBMIP (Fettweis et al., 2020; Krebs-Kanzow et al., 2020). The importance of high resolution of the ocean model in coastal and near coastal regions, which is available via the oceanic components in AWI-ESM1 and AWI-ESM2, for a realistic simulation of the impact of freshwater perturbations on the AMOC has been demonstrated (Lohmann et al., 2020). We have also studied importance of a salty deep ocean towards glacial termination (Knorr et al., revised).

The collapse of the ice sheets of the northern hemisphere during the last ice age affected the hydrological balance at high latitudes in the North Atlantic and thus the ocean circulation after the last ice age. Surprisingly, geological data suggest that meltwater flows of about 14-20 m sea level equivalent were washed into the North Atlantic without significantly affecting the Atlantic meridional circulation. Global reconstructions of sea level indicate abrupt changes within several hundred years and a rise in sea level during the Bølling/Allerød warming interval (Clark et al., 1996, 2002). Using our high-resolution climate model near the coast, we have studied the response of ocean circulation to deglacial freshwater discharges (Lohmann et al., 2020). In our experiments we find a high sensitivity of the ocean circulation depending on where the deglacial meltwater is injected (Figure 5).

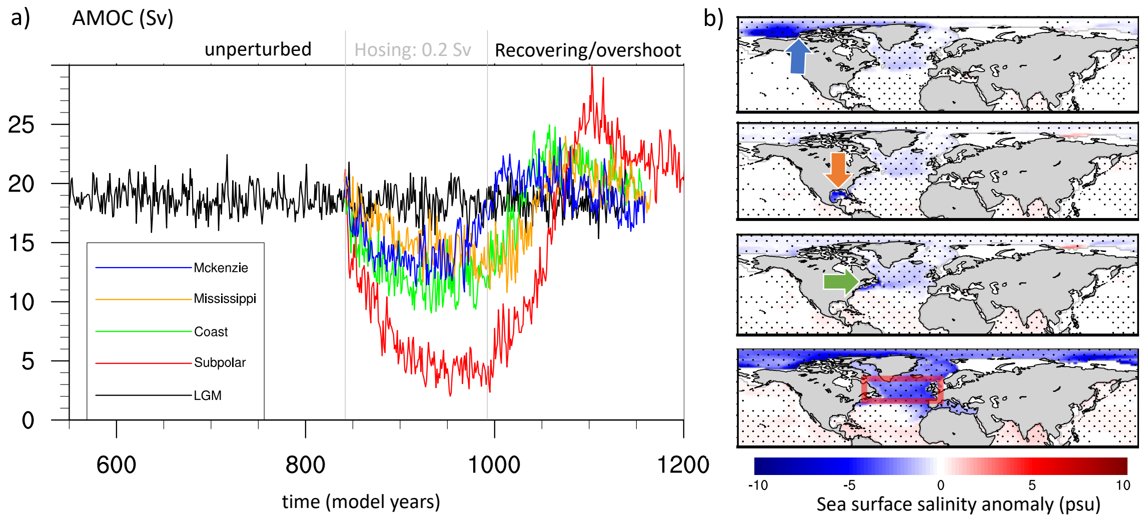

Figure 5: a) AMOC indices in the North Atlantic for different meltwater scenarios with AWI-ESM. The black line represents the undisturbed LGM experiment. b) Annual mean sea surface salinity anomaly between LGM and the sturgeon experiment LGM with 0.2 Sv for the model years 900-950. The dotted areas are significant at a confidence level of 95% (t-test). Figure taken from Lohmann et al. (2020*).*

Meltwater discharges across the Mississippi and near the coast of Labrador have little impact on AMOC. The reduced sensitivity of the overturning circulation to freshwater disturbances along the Mississippi route provides a consistent picture of deglacial climate development. However, a reduction in the salt concentration of the subpolar North Atlantic, which mimics water transport through icebergs, leads to a quasi-shutdown of the AMOC. Therefore, fresh water injection is more effective during Heinrich events. Future model developments should therefore focus on modelling ice calving and iceberg transport in the ocean (Rackow et al., 2018; and section below).

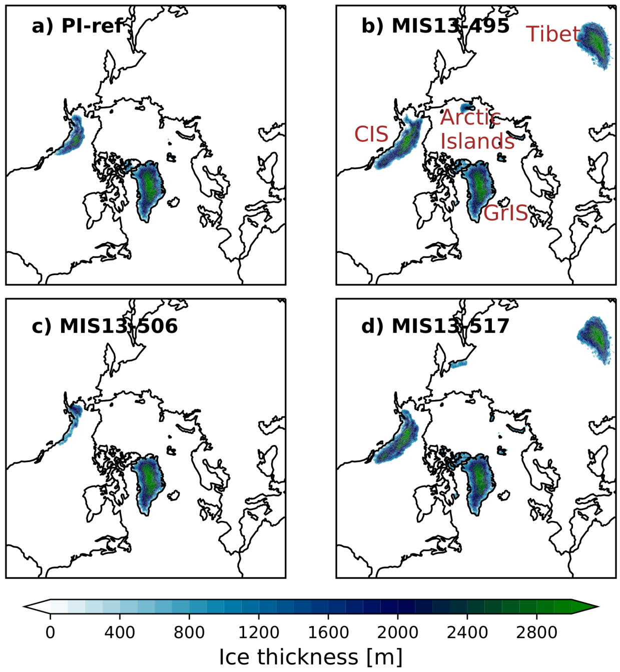

Figure 6: The simulated ice thickness under different orbital configurations at different time slices as simulated with AWI-ESM-1.2: (a) PI-ref, (b) MIS13-495, (c) MIS13-506, (d) MIS13-517.

Towards an understanding of the sensitivity of the Cordilleran ice sheet to precession and carbon dioxide forcing we simulated climate and Northern Hemisphere ice sheet evolution during MIS-13 employing three different astronomical configurations at 495, 506 and 517 kyr BP by means of AWI-ESM1.2 (Niu et al., submitted). At intermediate levels of carbon dioxide the Cordilleran Ice Sheet is more sensitive to orbital (precession) forcing (Figure 6). Due to internal ice sheet-climate feedbacks dynamic surges of the Cordilleran Ice Sheet occur under equilibrium forcing.

The future warming scenario RCP8.5 has been simulated with AWI-ESM1.2 (Ackermann et al., 2020). It has been found that the AMOC recovers after an initial slowdown in runs with and without the interactive ice sheet. Surface accumulation on the ice sheet partly compensates for the melt-induced freshwater release. Hence, the ice sheet acts as both a source and a sink for freshwater and adds strong decadal variability to the freshwater release. Related to this finding we note that an iceberg model (Figure 7) is included in AWI-ESM2.2. Freshwater and heat fluxes are coupled between the ocean and iceberg model, allowing for simulating the effects of iceberg melting on ocean dynamics. The coupling with PISM enables the iceberg initialization in regions with high discharge rates. A scaling approach is used to reduce the total number of icebergs and hence the computation time, in which a single simulated iceberg represents several icebergs.

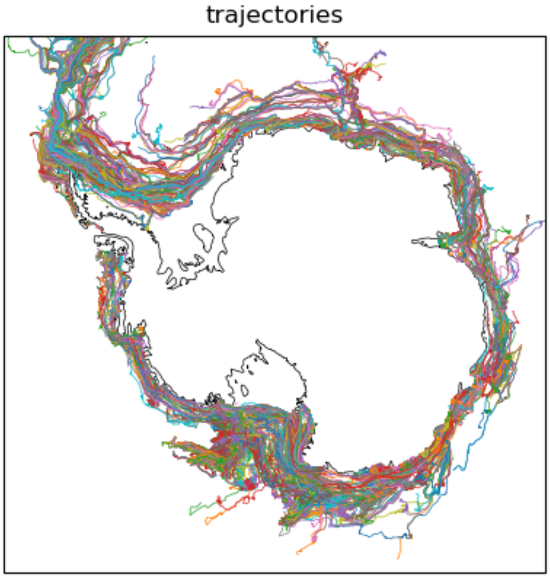

Figure 7: Trajectories of ice bergs around Antarctica computed by an ice berg model that is being coupled to AWI-ESM2.2.

1.2 References

Ackermann, L., Danek, C., Gierz, P., and Lohmann, G.: AMOC recovery in a multicentennial scenario using a coupled atmosphere-ocean-ice sheet model, Geophys. Res. Lett., 47, e2019GL086810, https://doi.org/10.1029/2019GL086810, 2020.

Bagge, M., Klemann, V., Steinberger, B., Latinović, M., Thomas, M.: Glacial-isostatic adjustment models using geodynamically constrained 3D Earth structures, Geochem., Geophys., Geosys, in prep. for resubmission, 2020.

Barbi, D., Wieters, N., Gierz, P., Chegini, F., Khosravi, S., and Cristini, L.: ESM-Tools Version 4.0: A modular infrastructure for stand-alone and coupled Earth System Modelling (ESM), Geosci. Model Dev. Discuss., https://doi.org/10.5194/gmd-2020-100, in review, 2020.

Clark, P. U., Alley, R. B., Keigwin, L. D., Licciardi, J. M., Johnsen, S. J., and Wang, H: Origin of the first global meltwater pulse following the Last Glacial Maximum, Paleoceanography, 11, 563–577, https://doi.org/10.1029/96PA01419, 1996.

Clark, P. U., Mitrovica, J. X., Milne, G. A., and Tamisiea, M. E.: Sea-level fingerprint as a direct test for the source of global meltwater pulse 1A, Nature, 295, 2438–2441, https://doi.org/10.1126/science.1068797, 2002.

Danilov, S., Sidorenko, D. Wang, Q., and Jung, T.: The Finite-volumE Sea ice–Ocean Model (FESOM2), Geosci. Model Dev., 10, 765-789, https://doi.org/10.5194/gmd-10-765-2017, 2017.

Fettweis, X., Hofer, S., Krebs-Kanzow, U., Amory, C., Aoki, T., Berends, C. J., Born, A., Box, J. E., Delhasse, A., Fujita, K., Gierz, P., Goelzer, H., Hanna, E., Hashimoto, A., Huybrechts, P., Kapsch, M.-L., King, M. D., Kittel, C., Lang, C., Langen, P. L., Lenaerts, J. T. M., Liston, G. E., Lohmann, G., Mernild, S. H., Mikolajewicz, U., Modali, K., Mottram, R. H., Niwano, M., Noël, B., Ryan, J. C., Smith, A., Streffing, J., Tedesco, M., van de Berg, W. J., van den Broeke, M., van de Wal, R. S. W., van Kampenhout, L., Wilton, D., Wouters, B., Ziemen, F., and Zolles, T.: GrSMBMIP: Intercomparison of the modelled 1980–2012 surface mass balance over the Greenland Ice sheet, The Cryosphere Discuss., https://doi.org/10.5194/tc-2019-321, accepted for publication in The Cryosphere, 2020.

Gierz, P., Ackermann, L., Rodehacke, C. B., Krebs-Kanzow, U., Stepanek, C., Barbi, D., and Lohmann, G.: Simulating interactive ice sheets in the multi-resolution AWI-ESM 1.2: A case study using SCOPE 1.0, Geosci. Model Dev. Discuss., https://doi.org/10.5194/gmd-2020-159, in review, 2020.

Gowan, E.J., X. Zhang, S. Khosravi, A. Rovere, P. Stocchi, A. L. C. Hughes, R. Gyllencreutz, J. Mangerud, J. I. Svendsen, and G. Lohmann: A new global ice sheet reconstruction for the past 80,000 years. Nature comm. (revised), 2020.

Kageyama, M., Harrison, S. P., Kapsch, M.-L., Löfverström, M., Lora, J. M., Mikolajewicz, U., Sherriff-Tadano, S., Vadsaria, T., Abe-Ouchi, A., Bouttes, N., Chandan, D., LeGrande, A. N., Lhardy, F., Lohmann, G., Morozova, P. A., Ohgaito, R., Peltier, W. R., Quiquet, A., Roche, D. M., Shi, X., Schmittner, A., Tierney, J. E., and Volodin, E.: The PMIP4-CMIP6 Last Glacial Maximum experiments: preliminary results and comparison with the PMIP3-CMIP5 simulations, Clim. Past Discuss., https://doi.org/10.5194/cp-2019-169, in review, 2020.

Knorr, G., S. Barker, X. Zhang, G. Lohmann, X. Gong, P. Gierz, C. Stepanek, and L. Stap: A salty deep ocean as a prerequisite for glacial termination, Nature Geo., revised, 2020.

Koldunov, N. V., Aizinger, V., Rakowsky, N., Scholz, P., Sidorenko, D., Danilov, S., and Jung, T.: Scalability and some optimization of the Finite-volumE Sea ice-Ocean Model, Version 2.0 (FESOM2), Geosci. Model Dev., 12, 3991-4012, https://doi.org/10.5194/gmd-12-3991-2019, 2019.

Krebs-Kanzow, U., Gierz, P., Rodehacke, C. B., Xu, S., Yang, H., and Lohmann, G.: The diurnal Energy Balance Model (dEBM): A convenient surface mass balance solution for ice sheets in Earth System modeling, The Cryosphere Discuss., https://doi.org/10.5194/tc-2020-247, in review, 2020.

Lohmann, G., Butzin, M., Eissner, N., Shi, X., and Stepanek, C.: Abrupt climate and weather changes across time scales, Paleoceanogr. and Paleoclimatol., 35, e2019PA003782, https://doi.org/10.1029/2019PA003782, 2020. Special Section AGU Grand Challenges in the Earth and Space Sciences.

Niu, L., Lohmann, G., Gierz, P., Gowan, E. J., and Knorr, G.: Coupled climate-ice sheet modelling of MIS-13 reveals a sensitive Cordilleran Ice Sheet, Glob. Planet. Change, submitted.

Otto-Bliesner, B. L., Brady, E. C., Zhao, A., Brierley, C., Axford, Y., Capron, E., Govin, A., Hoffman, J., Isaacs, E., Kageyama, M., Scussolini, P., Tzedakis, P. C., Williams, C., Wolff, E., Abe-Ouchi, A., Braconnot, P., Ramos Buarque, S., Cao, J., de Vernal, A., Guarino, M. V., Guo, C., LeGrande, A. N., Lohmann, G., Meissner, K., Menviel, L., Nisancioglu, K., O'ishi, R., Salas Y Melia, D., Shi, X., Sicard, M., Sime, L., Tomas, R., Volodin, E., Yeung, N., Zhang, Q., Zhang, Z., and Zheng, W.: Large-scale features of Last Interglacial climate: Results from evaluating the lig127k simulations for CMIP6-PMIP4, Clim. Past Discuss., https://doi.org/10.5194/cp-2019-174, in review, 2020.

Rackow, T., Wesche, C., Timmermann, R., Hellmer, H. H., Juricke, S., and Jung, T.: A simulation of small to giant Antarctic iceberg evolution: Differential impact on climatology estimates, J. Geophys. Res. Oceans, 122, 3170–3190, https://doi.org/10.1002/2016JC012513, 2018

2. Project 1030

Project title: PalMod WG2
Project lead: Victor Brovkin
Subproject lead: Peter Köhler (WP2.1, AWI), Birgit Schneider (WP2.1, CAU Kiel), Tatiana Ilyina (WP2.1, MPI-M), Victor Brovkin (WP2.2, MPI-M), Thomas Kleinen (WP2.3, MPI-M), and Benedikt Steil (WP2.3, MPI-C)
Allocation period: 2020-01-01 to 2020-09-31

PalMod is a BMBF-funded project focused on understanding earth system dynamics and variability during the last glacial cycle. The first phase of PalMod ran from 2015-08-01 to 2019-07-31 and focused on the time from the Last Glacial Maximum to the present. The second project phase runs from 2019-10-01 to 2022-09-30 and will revisit the deglaciation, but also investigate the glacial inception and the strong variability during Marine Isotope Stage 3.
WG2 of PalMod aims at understanding and quantifying feedbacks between biogeochemistry and climate during glacial cycles. Three work packages are focusing on the marine carbon cycle, terrestrial processes, and the CH_4 cycle. Scientific challenges include reproducing the glacial CO_2 cycle with comprehensive ESMs, understanding of rapid changes in atmospheric greenhouse gas concentrations during abrupt climate changes, and reconstructing the atmospheric lifetime of CH_4 using a coupled atmospheric chemistry model.
PalMod WG2 contains work packages WP2.1 “Marine carbon cycle“, WP2.2 “Terrestrial carbon cycle”, and WP2.3 ”Methane cycle”. During the reporting period all work packages requested computation time from DKRZ.

2.1 Situation of PalMod II WG2 in 2020

2020 was a difficult year due to the COVID19 pandemic. The main impact on PalMod and thus project bm1030 was that several positions could not be filled timely, especially in cases where candidates from abroad were to be hired, as these could not enter Germany for several months. As a result, work in some parts of bm1030 was strongly delayed, and work on one part (WP 2.1, Alfred Wegener Institut) has been delayed so severely that no computation time could be used and no work on the project can be reported ti this date.
Further project delays due to the COVID19 pandemic were related to the closure childcare facilities for several months, severely impacting the ability of project members to work and the general difficulties of communicating when not being able to come to the office.
In addition, WP2.1 (MPI-M) and WP2.3 (MPI-C) experienced some technical difficulties, as detailed below.

WP2.1 (MPI-M)

Unfortunately, we experienced delays in many of the simulations planned for 2020 due to following reasons. First, we encountered unexpected technical issues in the transient deglaciation simulation with regard to the changing ocean bathymetry and coastlines due to melt water input. In particular, extreme salinities (>200 psu or negative values) occur during the automatic creation/removal of some ocean grids, which lead to unrealistic values of salinity-dependent biogeochemical parameters and therefore the crash of the model. Such issues are supposed to be tackled by a colleague in the subproject CC.1SP3. However, this position was vacant for eight months (Sep 2019 – April 2020) until a new postdoc had been hired. Thus, so far we performed only one deglaciation simulation. The other two transient deglaciation runs planned for 2020, one with another ice sheet reconstruction ICE-6G and the other with temporally-varying weathering input, will be performed in year 2021.

Second, we have to implement a new radiocarbon ^{14}C module in the ocean biogeochemical component HAMOCC because the ^{14}C module previously implemented in the ocean physical component MPIOM is based on the CMIP5 version of MPI-ESM and it does not work in our current model set-up based on the CMIP6 version of MPI-ESM. Third, after some recent updates in HAMOCC (i.e., the inclusion of temperature-dependent POM remineralisation; accounting for DOM degradation in low oxygen conditions), the simulated oceanic N:P ratio became too low for present-day ocean (12 in the model compared to about 16 in observations) and thus required further parameter tuning. In 2020 we performed 4 simulations of the 15 planned time-slice simulations which were designed to investigate the sensitivity of ocean biogeochemistry to different physical and biological conditions during LGM. We additionally performed 4 sensitivity simulations (that was not planned prior to 2020) regarding to cloud parameters, based on the recent outcome of model tuning performed by subproject WP1.1SP3. Due to the third issue mentioned above, we have stopped the time-slice runs and we are currently analysing and adjusting some HAMOCC parameters. The not finished/performed time slice simulations will be conducted in year 2021.

Finally, the COVID-19 pandemic has noticeably slowed down our progress due to the challenges of the working conditions of home offices, and due to less efficient communication between colleagues.

WP2.3 (MPI-C)

Due to an incorrect setting in the model run-scripts, several large simulations with EMAC were accounted on the balance of MPI-C (mm0062, MINOS project) instead of PalMod (bm1030) in 2020. These amount to 43599/47721/53559 [Node hours] of Mistral computing time and 716/2533/5775 [GiB] of Lustre work in April/June/July 2020, respectively. The job numbers/logs of these erroneously accounted simulations are available.

2.2 Report on Resources used in 2020

WP 2.1 “Marine carbon cycle“, CAU Kiel

2020 was an unusual year for us, and many things did not go as planned, also with respect to the computations at DKRZ that we had envisaged.

In winter 2019 and spring 2020, we implemented the marine particle ballasting scheme (that we had earlier tested in the ocean-only setup MPIOM/HAMOCC) in MPI-ESM. More specifically, we used the land-atmosphere-ocean setup of MPI-ESM that has already been used by Thomas Kleinen at MPI-M for transient deglaciation simulations. Note, however, that those runs were performed without HAMOCC. Within this setup, we re-tuned HAMOCC with the ballasting scheme, and performed, as planned, PI and LGM time-slice experiments to gain first insights into marine particle ballasting differences (Figure 1).

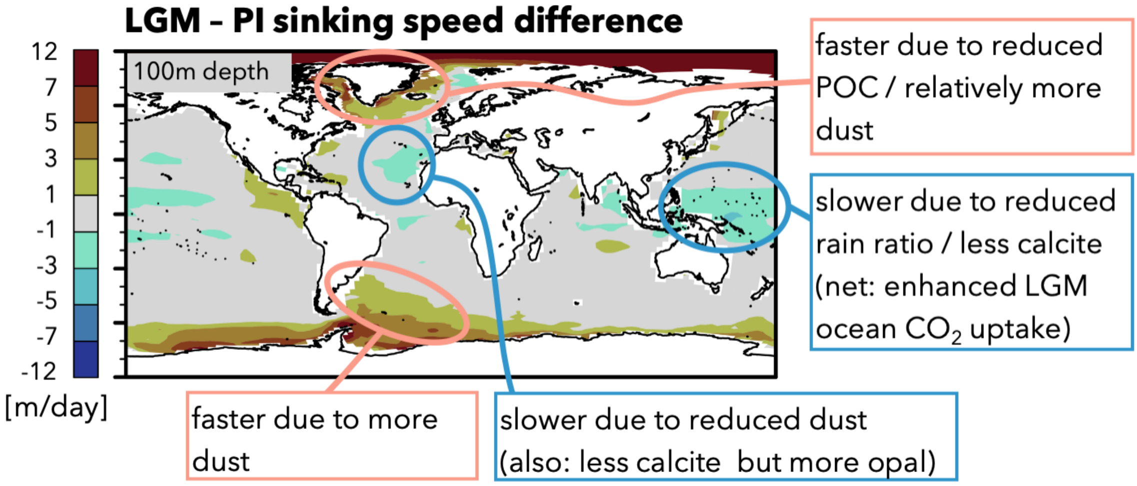

Figure 1: LGM-PI sinking speed differences at 100m depth, based on 1000-year-long LGM and PI MPI-ESM time-slice experiments, and the respective reasons for the LGM anomalies.

To quantify the effect of ballast changes on the atmospheric pCO_2 drawdown during the last deglaciation, we had further planned to perform transient MPI-ESM deglaciation simulations after these time-slice experiments. Unfortunately, HAMOCC was not ready for these transient simulations due to several reasons. The two most important reasons are, first, technical difficulties, which arose from the interactive HAMOCC land-sea mask, led to too high or negative salinities during grid generation, and eventually caused HAMOCC to crash. And second, the position that was supposed to tackle this and other HAMOCC issues was vacant for 8 months from September 2019 until April 2020 (see also report by WG2.1 MPI-M). However, since it was not predictable when the HAMOCC code would be ready for the transient simulations, we remained hopeful to still be able to run them, in particular since those simulations are our main PalMod deliverable. Note that 2 of the (originally planned 3) transient simulations require 2x30000 coarse resolution MPI-ESM simulation years equivalent to about 60000 node hours, which is most of the computation time that we were granted for this year (63168 node hours).

As an alternative tool to perform the promised transient deglaciation simulations with HAMOCC and our ballasting scheme, we started to port the EMIC ClimberX (developed at PIK, including HAMOCC) to Mistral. But unfortunately, by then, the Covid-19 crisis had already started. It had led to the lack of daycare (Kita) for the 2-

year-old daughter of the postdoc for 5 months, from March 16th 2020 until August 17th 2020, which significantly slowed down the progress made in the home office, so that we do not have any ClimberX results to show yet.

Additionally, the postdoc is now on parental leave for a second child that was born on August 4th 2020. Therefore, we are now planning to shift the transient simulations originally planned for 2020 into the year 2021.

WP 2.1 "Marine carbon cycle", MPI-M

Transient deglaciation simulation with ocean carbon cycle

In 2020 we performed our first transient deglaciation simulation with the ocean carbon cycle in MPI-ESM and started to analyse model output. We have to note that in this process we had to tackle and resolve some unexpected technical issues related to changing ocean bathymetry and coastlines due to melt water input, such as extremely high salinities >200 psu or negative salinities (detailed in Section "Usage of computing time in 2020"). Thus, our first focus was to understand how ocean biogeochemistry responds to deglacial changes of the climate and ocean physics. In particular, we quantified the mechanisms affecting surface ocean pCO2. We also use our newly developed comprehensive stable carbon isotope ^{13}C module to compare to paleo $\delta^{13}C$ record from sediment core to evaluate the simulated ocean states.

During deglaciation AMOC stays strong (except for the period of massive melt water discharge, Fig 2a) and the strength of upwelling in the Southern Ocean is relatively stable. As a result, our first analysis shows that the often-hypothesized mechanism that the deglacial atmospheric CO2 rise is caused by enhance ocean ventilation is not supported in our current model set-up. Other deglacial changes, such as the decreased solubility with increasing sea surface temperature, decreased surface alkalinity (Fig 2c) due to melt water input and episodically increased biological CaCO3 production, are not effective enough to elevate surface pCO2. Thus, the ocean is a weak CO2 sink (Fig 2b). In the North Atlantic, the model captures the $\delta^{13}C$ decline during a massive melt water input (Fig 2d). The timing of this $\delta^{13}C$ decline is later than in the sediment record because the Heinrich Stadial is not well represented in the model. In the Southern Ocean, the observed $\delta^{13}C$ increases after 15 ka BP, suggesting increased ventilation, which is not captured by the model (Fig 2e).

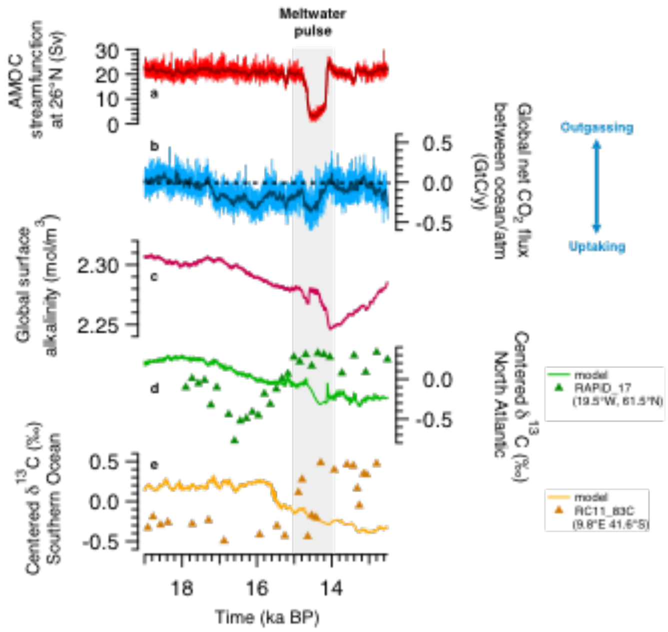

Figure 2: Time evolution of the AMOC strength (a), the global net CO2 flux between ocean and atmosphere (b, positive into atmosphere), the global mean surface alkalinity (c) the centered $\delta^{13}C$ (removing the long-term means) of the model and sediment core record at 2300 m depth in the North Atlantic Ocean 19.5W 61.5N (d) and at 4000 m depth in the South Atlantic Ocean 9.8E 41.6S (e) in a transient deglacial simulation. The model is forced by reconstructions of atmospheric greenhouse gas concentrations, orbital parameters, ice sheet and dust deposition.

Oceanic ^{13}C Suess effect

Another focus of our studies in 2020 is to finalize the analysis and the corresponding manuscript on the development and evaluation of the new 13C module in HAMOCC, which explicitly resolves 13C for all existing oceanic carbon pools and fractionation during air-sea gas exchange and for biological fractionation associated with photosynthetic carbon fixation during phytoplankton growth are accounted for. A novel aspect of this work is with our consistent model framework we quantify the uncertainties in the approach of Eide et al. (2017) which produces the first observation-based estimate of the global ocean 13C Suess effect ($\delta^{13}C_{SE}$) since pre-industrial times. The later study assumes linear relationships between $\delta^{13}C_{SE}$ and pCFC12 (Chlorofluorocarbon-12 partial pressure) and assumes the proportionality factors are the same with those between preformed $\delta^{13}C$ ($\delta^{13}C_{pref}$) and pCFC12 (both measured in the present-day ocean). We find the Eide approach is likely to underestimate $\delta^{13}C_{SE}$ in the Indian Ocean, as is illustrated by a less negative proportionality factor for $\delta^{13}C_{pref}$ - pCFC12 relationship than that for $\delta^{13}C_{SE}$ - pCFC12 (Fig3a and 3c). This is mainly due to a positive correlation between the $\delta^{13}C_{pref}$ prior to industrial times and pCFC-12 in the present-day ocean, which is neglected in the Eide approach. We also find this potential underestimation in the North Pacific and the South Atlantic Ocean (not shown). In the North Atlantic Ocean, the Eide approach is likely to overestimate $\delta^{13}C_{SE}$ because the changes in the ocean carbon cycle and the increased isotopic fractionation during phytoplankton growth under increased surface pCO2 are neglected (Fig 3b and 3d).

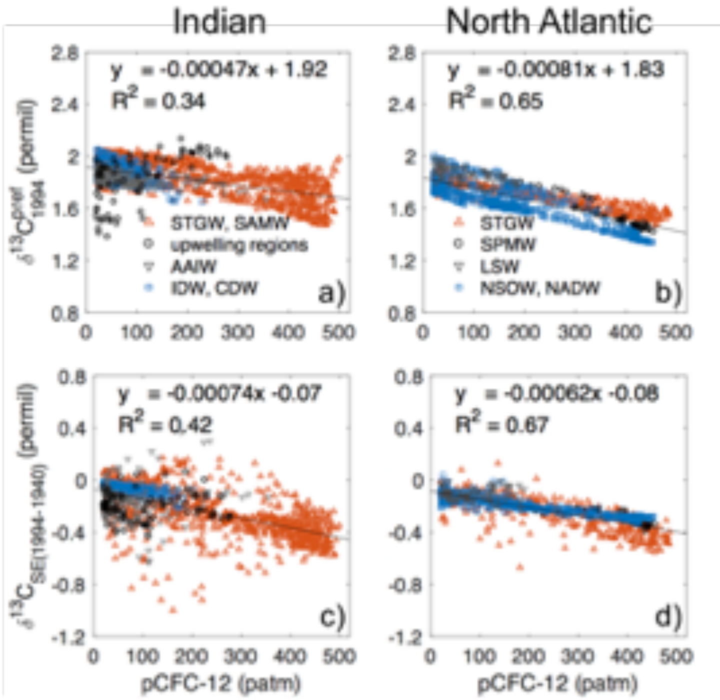

Figure 3: Relationship between pCFC-12 and $\delta^{13}C_{pref}$ for the Indian Ocean (a) and the North Atlantic Ocean (b). (c, d): as a and b, but for the relationship between pCFC-12 and $\delta^{13}C_{SE(1994\text{-}1940)}$.

WP2.2 "Terrestrial Carbon Cycle", MPI-M

For 2020, WP2.2 had originally planned to perform factor separation experiments for the deglaciation, with one experiment driving the model completely with observed CO_2, one experiment driving model physics with observed CO_2, but using interactive CO_2 for the biogeochemistry, and one experiment using completely interactive biogeochemistry. A further planned focus were the first glacial inception experiments.

The latter experiments have not yet been performed, but they are are still envisioned for the last quarter of 2020. For the factor separation experiments, however, we came to the realisation that the marine carbon cycle in MPIESM was not yet sufficiently calibrated in early 2020 for these experiments to take place as planned. We did conduct two of these experiments, using two different weathering parameterisations in order to increase C storage in the glacial ocean, but we had to abort them after about 10000 model years, as oceanic C changes were much smaller than required by ice-core reconstructions of atmospheric CO_2.

In addition, to these (aborted) experiments, we investigated the transfer of land carbon into the oceanic domain, as the sea level rises during the deglaciation, as well as the effect of anthropogenic land-use changes on the terrestrial C cycle.

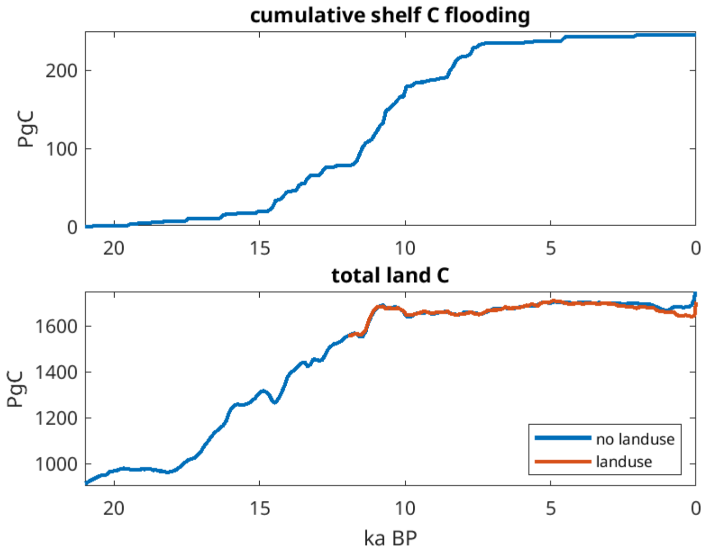

Figure. 4: (Top) Carbon transferred from terrestrial to ocean domain due to flooding of shelf areas. (Bottom) total carbon on land, without(blue) and with(orange) anthropogenic land use.

During the deglaciation, a total of nearly 250 PgC is transferred from the shelf areas to the oceanic domain, as land is flooded during sea level rise. This is substantially more carbon than the LGM carbon storage on the shelves, as terrestrial productivity increases before the shelves are flooded. In comparison to the increase in total land C, which sets in at about 18 ka BP and continues to 11 ka BP, the C transfer from the shelf areas to the ocean starts at about 15 ka BP, but continues until about 8 ka BP (Fig. 4).

By imposing the HYDE data set of anthropogenic land use, which reconstructs land use from 1000 BC to the present, we could also assess the effects of anthropogenic land use on the terrestrial carbon cycle (the Ruddiman hypothesis). In comparison to the baseline experiment without landuse, the total terrestrial carbon storage is only slightly decreased, implying negligible effects on atmospheric CO_2 (Fig. 4).

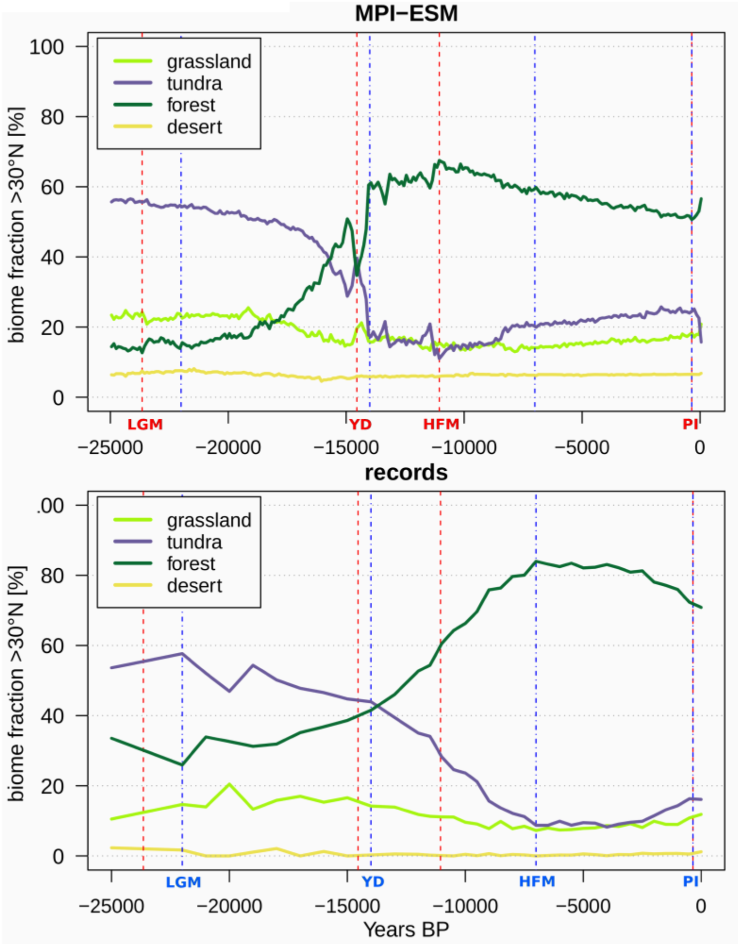

Figure 5: (Top) Biomes as assessed from MPIESM plant functional types, (Bottom) Biomes as reconstructed from Pollen data. Comparison for areas north of 30°N.

As our methodology for assessing modelled vegetation in comparison to proxy data has advanced (Dallmeyer et al., 2019), we were also finally able to assess the quality of the modelled vegetation, as compared to biome reconstructions from pollen data (Fig. 5). While model and reconstructions are in decent agreement for tundra and desert, the model underestimates forest area and overestimates temperate grasslands. Also, forest expansion during the deglaciation sets in substantially earlier in the model than in the reconstructions. Some part of this discrepancy in timing is well understood (vegetation by design spreads much faster in the model), but the overall discrepancy requires further analysis.

WP 2.3 “Methane cycle” (MPI-M)

In 2020, we finalised the publication on time slice experiments we had worked on in previous years. In addition to the work on this model description publication (Kleinen et al., 2020), we investigated the methane cycle further, for the deglaciation, for the Bølling-Allerød / Younger Dryas transition, and for future climate conditions. We also continued work on the atmospheric sink of methane, refining the estimate of CH_4 lifetime by determining biospheric emissions of reactive Carbon and reactive Nitrogen, in addition to the NO_x emissions by lightning.

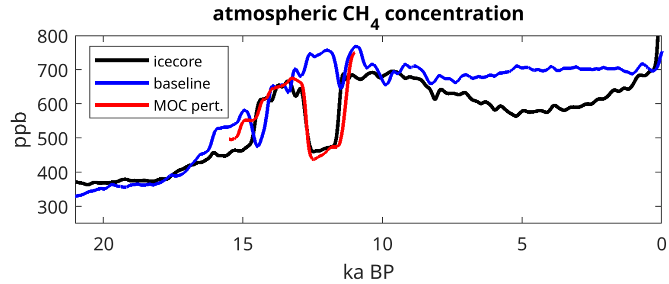

Figure 6: Atmospheric concentration of CH_4 in ice core, baseline MPIESM experiment, and MOC perturbation experiment.

Using the same transient model experiment of the deglaciation, we further investigated the natural methane cycle. The baseline experiment (Fig. 6, blue) is unable to reproduce the ~150 ppb drop in atmospheric CH_4 apparent in the ice core reconstruction. In order to improve the situation, we performed a set of AMOC perturbation experiments, as previous experiments (see report 2019) had shown that an AMOC perturbation has a similar signature in terms of atmospheric methane as the Bølling-Allerød / Younger Dryas transition. The final experiment configuration (Fig. 6, red) displays a methane signature very similar to the ice core signal of the BA/YD transition, in addition to a Younger Dryas period of suitable length.

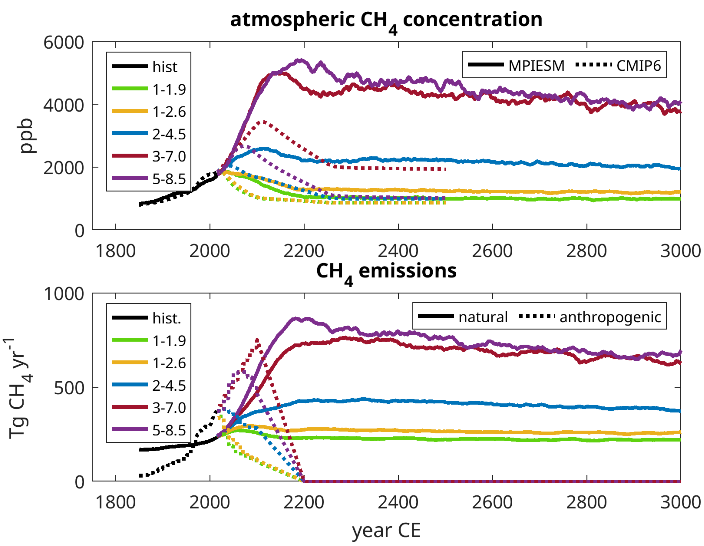

Figure 7: Extension of transient deglaciation experiment into the future for SSP scenarios. (Top) atmospheric CH_4 concentration, (bottom) natural and anthropogenic CH_4 emissions.

Extending the deglaciation experiments into the future, we are able to show that the CMIP6 scenarios strongly underestimate future atmospheric methane (manuscript in preparation). While Meinhausen et al. (2020) assume that natural emissions of methane will remain constant in the future, our experiments show that these will increase strongly (Fig. 7), leading to atmospheric concentrations of methane well above those contained in the CMIP6 scenarios.

WP 2.3 "Methane cycle" (MPI-C)
Atmospheric oxidative capacity and climate variations

Within the project year 2020, we have continued numerical experiments using comprehensive atmospheric chemistry simulations with the EMAC model, targeting the improvement of the atmospheric CH4 removal parametrisation used in time-slice/transient simulations with MPI-ESM. More specifically, (1) the role of atmospheric aerosol burden (AB) on reducing atmospheric oxidative capacity was estimated, (2) the CH_4atmospheric reactivity (or equivalently lifetime) fit parameters were re-evaluated, and (3) estimates/calibration of the surface sources magnitudes for transient (deglaciation) runs was performed.
Regarding (1), the effect of aerosol on atmospheric oxidative capacity (hence CH_4 lifetime, τ_{CH4}) in our models was not reckoned explicitly to date. The sensitivity simulations with AB removed from the troposphere suggest similar effect for τ_{CH4}in both, PD and LGM (4−6%, respectively). To a great extent, this is explained by the fact that we use identical AB in both climate states (as prescribed in the PMIP-3 protocol followed in models setup). On the other hand, much greater reactive nitrogen (RN) emissions from the surface in PD are expected to buffer OH radical more, resulting in its much weaker reduction in the PD. Such is not the case because of strong co-localization of the AB with the other sources (e.g. close to the surface), where OH buffering is suppressed. Furthermore, the effect is small for the CH_4 lifetime because most of CH4 sink occurs in the free troposphere. This is confirmed by the analysis of the τ_{CH4}fit, which yields best regression score when the AB term is added to the reactive carbon (RC) part (see below). Indirectly, this also suggest co-location of the AB and RC sources, that is, their likely alignment with the vegetation distribution. Accounting for the AB distribution, the updated τ_{CH4}fit is thus formulated as:

$$\tau_{CH4}^{-1} = a \cdot (LN + RN\cdot k_{RN})^{p} \cdot (M + RC\cdot k_{RC} + AB\cdot k_{AB})^{q}$$

where a, p, $q$and k are the fit constants for respective parameters, including CH_4burden (M) and nitrogen oxides (NO_X=NO+NO_2) emissions from lightning (LN).
Together with introduction of the AB component, τ_{CH4} fit was revisited regarding the choice of the proxy for the RN parameter. In contrast to EMAC, most of the models/studies to date do not implement/report emissions of N-bearing reactive compounds (RN) other than NO and NO_2, which makes inter-comparison of results more difficult. In an attempt to remedy this, we used only emitted surface NO_X as a proxy for the RN parameter, which resulted in an insignificant change of the fit quality (adj. R^2 changes within ±0.02 for reactivity or τ_{CH4}, values for both are above 0.93, n = 43).
Figure 8 shows the comparison of the simulated and fitted τ_{CH4}values in experiments with EMAC and relevant earlier studies. Fit parameters derived for EMAC are not compatible with about half of other estimates derived, however, using alternative models and for different climate states, which highlights the problem of unequal sensitivity of chemical mechanisms implemented in AC-GCMs to the latter and foremost tropospheric NO_X burden. A straightforward consequence of such is incongruent estimates of RC/RN and CH_4emissions between the studies, especially

for pre-industrial periods. Nonetheless, switching to NO_X as a proxy for RN may facilitate eliminating this inconsistency and help preparing less uncertain emission trajectories tied to proxies related only to nitrogen oxides. Whether changes in climate states generate pronounced (and matching the fit) variations in τ_{CH4} simulated with EMAC for the periods between LGM and PI remains to be seen in our planned time-slice experiments for the end-2020 until mid-2021.

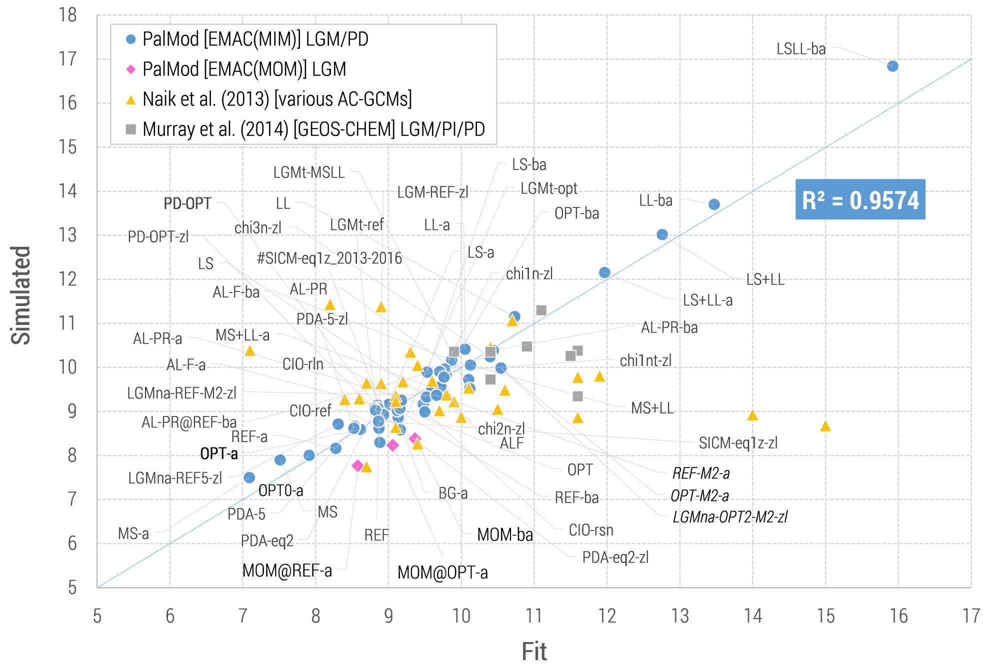

Figure 8. Fitted (abscissa) vs. simulated (ordinate) atmospheric CH_4 lifetime reckoned in experiments with EMAC (LGM and PD conditions, updated fit parametrisation using NO_X as the RN parameter) and in previous studies (various AC-GCMs and climate states, from LGM to PD). Points denote averages from single experiments, diamond symbols points denote experiments performed with the extended reference kinetic chemistry mechanism (MOM, computationally very expensive) exhibiting dependence similar to that of the optimum mechanism (MIM) conventionally used in EMAC.

2.3 Publications derived from bm1030

Kleinen, T. *et al.*: Terrestrial methane emissions from the Last Glacial Maximum to the preindustrial period. *Climate of the Past*, 16(2):575–595, 2020.

2.4 References

Dallmeyer, A. *et al.*: Harmonising plant funtional type distributions for evaluating Earth System Models. *Climate of the Past*, *15*, 335-366, 2019.

Kleinen, T. *et al.*: Terrestrial methane emissions from the Last Glacial Maximum to the preindustrial period. *Climate of the Past*, 16(2):575–595, 2020.

Meinshausen, M. *et al.*: The shared socio-economic pathway (SSP) greenhouse gas concentrations and their extensions to 2500. *Geoscientific Model Development*, 13(8):3571–3605, 2020.

Murray, L. T. *et al.*: Factors controlling variability in the oxidative capacity of the troposphere since the Last Glacial Maximum, *Atmos. Chem. Phys.*, **14**, 3589−3622, doi: 10.5194/acp-14-3589-2014, 2014.

Naik, V. *et al.*: Preindustrial to present-day changes in tropospheric hydroxyl radical and methane lifetime from the Atmospheric Chemistry and Climate Model

Intercomparison Project (ACCMIP), *Atmos. Chem. Phys.*, **13**, 5277−5298, doi: 10.5194/acp-13-5277-2013, 2013

3. Project 1029

Project title: PalMod WG3
Project: PalMod II - WP 3.3 - TP2 (explicit simulation of water isotopes with AWI-ESM)
Project lead: Martin Werner
Allocation period: 2020-01-01 to 2020-09-30

3.1 Report on resources used in 2020 in CC1

In the year 2020, WG3 resources had been asked for one subproject, only (WP3.3-TP2). Unfortunately, none of the granted DKRZ resources could be used between January and September because of the following two reasons:
1) exchange of personnel:
The previous postdoctoral researcher, who worked on this subproject during PalMod Phase I, had left AWI at the end of 2019. The position could only be filled again on July 1st, 2020. Thus, the work on subproject WP3.3-TP2 was paused for the first six months of this year.
2) update of model code:
Since the project start in July 2020, the work on subproject WP3.3-TP2 2020 has been focussed on finalizing the isotope-enhanced version of the AWI-ESM2 model (fully-coupled setup ECHAM6 and FESOM2). One key step up of the model has been the switch to the ECHAM6 code release with a concurrent radiation scheme. This ECHAM model version was developed during PalMod Phase I and enables a substantial reduction of computing time for ECHAM6. As water isotopes tracers will increase the required ECHAM6 computing time by approx. 50%, it was decided to switch to the ECHAM model version with concurrent radiation scheme for AWI-ESM2-wiso, too. *All necessary isotope code transfer and initial testing was done on AWI's own smaller HPC system as this enabled a more efficient workflow during the model development and testing phase.* For this reason, no DKRZ resources have been used, so far. As the model upgrade is finalized and first test simulations look very promising (see next chapter), we expect to use DKRZ resources for production runs with AWI-ESM-wiso (e.g., PI-Ctrl, various paleoclimate simulations) very soon.

3.2 Short summary of achieved results

AWI-ESM2-wiso is the latest version of AWI-ESM2 enhanced by stable water isotope diagnostics (i.e. incorporation of stable water stable isotope tracers $H_2{}^{16}O$, $H_2{}^{18}O$ and HDO). As explained in the previous chapter, it is now based on the latest ECHAM6 version including the concurrent radiation scheme. Here, we show two plots of initial test simulations (all performed on the AWI HPC system) to demonstrate the readiness of the AWI-ESM2-wiso model setup for the planned PalMod production runs. These test simulations look very promising and we therefore apply for necessary DKRZ HPC resources to perform first PalMod II productions runs with AWI-ESM-wiso in the year 2021.

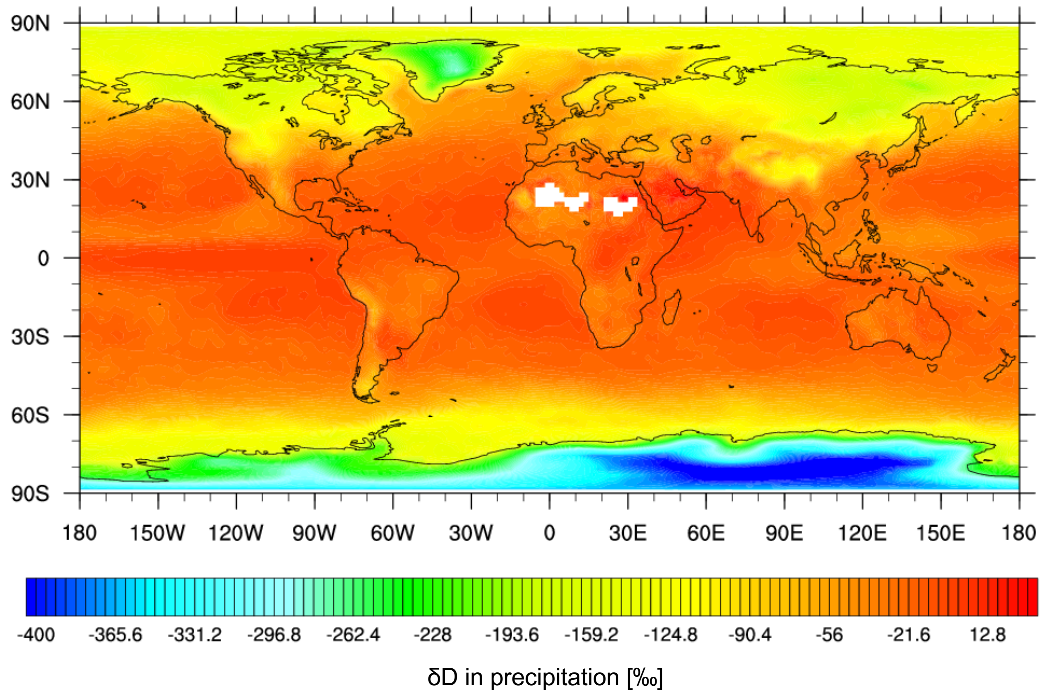

Figure 1: Global distribution of simulated annual mean δD values in precipitation under PI conditions, as simulated by a 1-year test experiments with the AWI-ESM2-wiso model setup. The global pattern of δD in precipitation shows all characteristic pattern (e.g., latitudinal gradients between subtropics and high latitudes, continental gradients over Eurasia and North America, strong isotope depletion over Greenland and Antarctica), similar to results achieved with the MPI-ESM-wiso model within PalMod

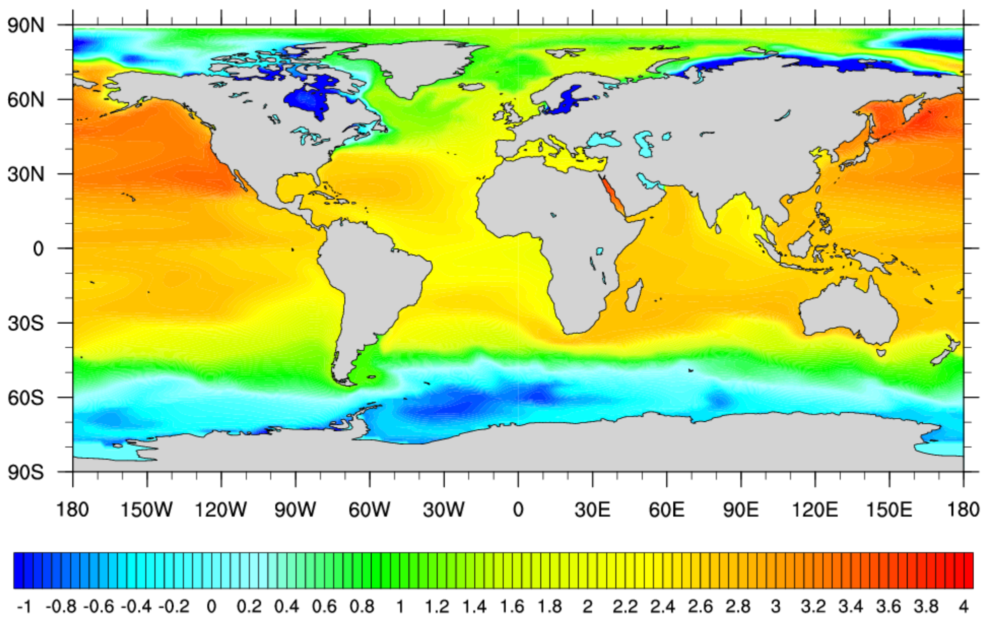

Phase I.

δD in ocean surface water [‰]

Figure 2: Global distribution of simulated annual mean δD values in ocean surface waters under PI conditions, as simulated by a 1-year test experiments with the AWI-ESM2-wiso model setup. The global pattern of δD in ocean surface water shows all characteristic pattern (e.g., latitudinal gradients between subtropics and high latitudes, different isotope enrichment in the Atlantic vs. Pacific Ocean, isotope depletion in the Arctic Ocean and the Antarctic Circumpolar Current region), similar to results achieved with the MPI-ESM-wiso model within PalMod Phase I.

4. Project 993

Project title: PalMod: A national paleo climate modelling initiative, cross-cutting activities (CC)
Project lead: Hendryk Bockelmann
Allocation period: 2020-01-01 to 2020-09-30

4.1 CC1: Report on resources used in 2020

WP CC.1-TP1– Enabling high throughput for coupled ESMs
As this subproject follows the aim to increase the integration rate of coupled ESMs within PalMod, we mainly used the resources to develop and test several optimisation approaches for the entire model setups used in WG1 and WG2 (Figure 2).

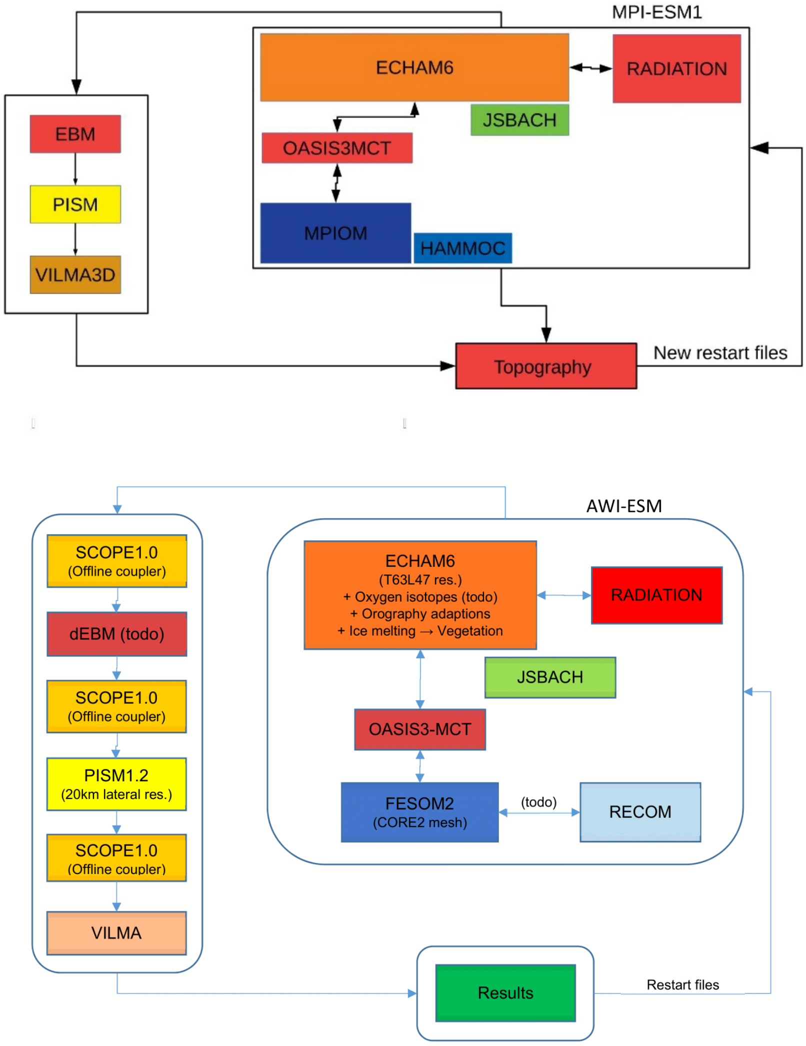

Figure 2: Whole model setup for common experiments of MPI-ESM and AWI-CM used in PalMod.

These steps are manifold and some are:

- Implementation and tuning of asynchronous radiation scheme in ECHAM6 used for coupled MPI-ESM PiControl experiments; also in preparation for AWI-CM

- Performance analysis of MPI-ESM using latest CDI-PIO and OASIS3MCT4.0 libraries
- Performance analysis of WP2.3 and WP1 experiments and integration of optimised models in PalMod experiments
- Model optimisation of topology adaptation and energy balance model
- hybrid MPI/OpenMP ECHAM6 debugging and performance analysis
- heterogeneous MPI-ESM (pure MPI MPIOM and hybrid MPI/OpenMP ECHAM6) debugging and performance analysis
- detailed analysis of VILMA model

All improvements and recommended setups for the mistral HPC-system (with regard to PalMod experiment settings) are reported on the website:

https://palmod.gitlab-pages.dkrz.de/modelperformance/

As an example of improved resource usage we'd like to mention the optimisation of EBM in MPI-ESM. The Energy Balance Model is the coupler between MPI-ESM and PISM/VILMA models. The standard model computes the ice sheet mass balance and the surface temperature over 24 elevation levels for every simulated year with MPI-ESM. The parallelisation is over the fixed 24 elevation levels, thus 24 cores in one node are used and the other nodes allocated to run the full ESM model are idling during EBM calculations. The calculations to evaluate the ice sheet mass balance and the surface temperature are done serially.

The optimised Energy Balance Model now computes the ice sheet mass balance and the surface temperature in parallel. In order to do that, two levels of parallelism are required. The higher level is given by the fixed 24 elevation levels, as in the standard model. The lower level computes the main calculations using an arbitrary number of cores. This means that on each node an arbitrary number of elevation levels are computed, so the code can be scaled on more than one node and the allocated resources can be fully exploited (Figure 3).

In total this optimisation leads to an improved peak performance of the model by a factor of 2.75 on the compute partition and of 2.5 on the compute2 partition on mistral.

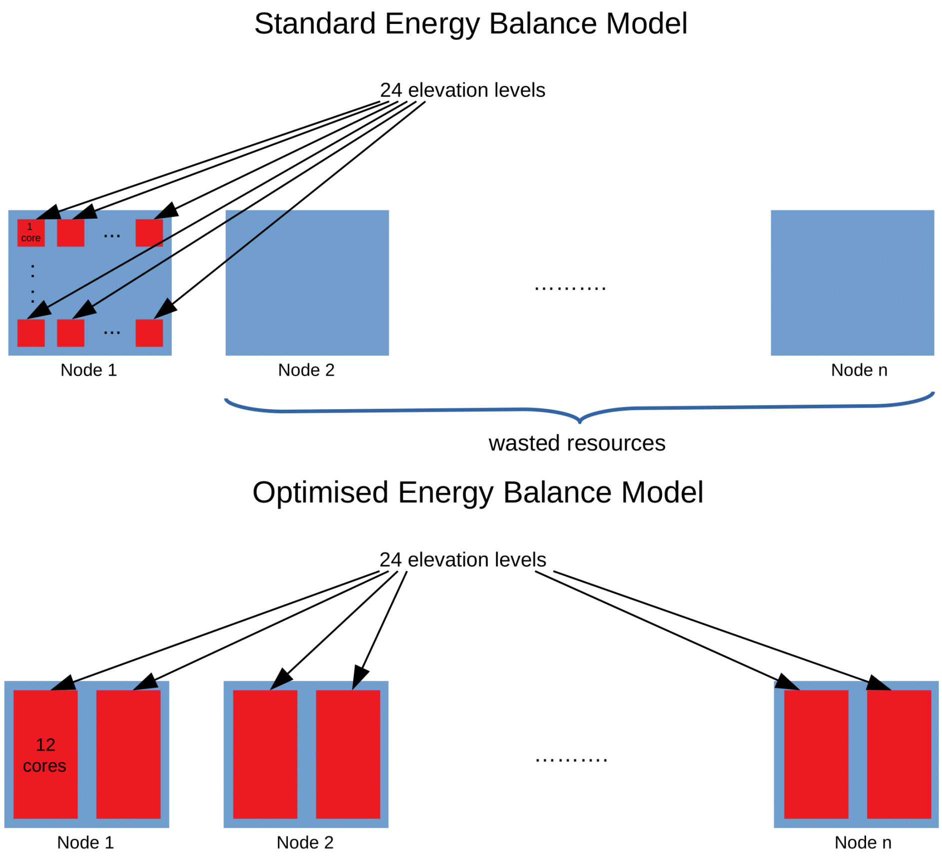

Figure 3: Optimisation of the Energy Balance Model to make better use of available compute resources.

WP CC.1-TP2 – Parallel-in-Time methods for ocean and climate simulations

We have to postpone main parts of the planned computer experiments to the last months of 2020 and to 2021. The student that was supposed to conduct the experiments could only work for some months. The chosen candidate turned out not to be able to come to the state where he was able to perform the planned runs independently. Due to the Corona situation, it was difficult to work in close (personal) cooperation and provide further assistance

WP CC.1-TP3– Paleo-lakes and hydrology on exposed shelves in MPI-ESM

The work on development of a dynamic lake model for MPI-ESM has been significantly delayed due to the unforeseen temporary diversion of work to other projects (ICON development and CLiCCS) thus the stage at which testing of the lake model within MPI-ESM was possible was only reached in November. Nevertheless, now the lake model has reach the point where it can run within transient runs. All work prior was done in a standalone setup and had a negligible computational cost (and was thus done on desktop machines). Hence the underutilization of compute time resources and storage this year.

WP CC.1-TP3 - Land-sea carbon and nutrient transfer related to sea level changes in MPI-ESM

Over the last years the global biogeochemical model HAMOCC has been technically adjusted to take into account a fully interactive adaptation of the ocean bathymetry with corresponding changes of the land-sea distribution and a transient river routing and the land-sea carbon. In collaboration with Working Group 2, fluxes of carbon and nutrients from land to the ocean during period of sea level change have been accounted for in HAMOCC. New tracers have been added to represent terrestrial organic matter inputs, i.e. terrestrial organic matter previously stored in different land compartments (woody biomass, litter, humus), in the water column and in the sediment. This guarantees a closed global carbon cycle and allows to account for the impact of terrestrial carbon fluxes on the ocean biogeochemical state over past climatic cycles.

A transient simulation over the last deglaciation is currently under progress (so far until 12 ka), which is the first transient simulation with a complex ESM. One of the goals of this simulation within this subproject is to investigate the potential impact of the terrestrial organic matter fluxes into the ocean on the global ocean biogeochemical cycle and the uptake/release of CO_2 during pronounced period of sea level change. The last deglaciation is characterized by periods of abrupt meltwater input to the ocean like the type of Heinrich event observed in the model between 15-14 ka and presented on Figure 1. These events are of particular interest to investigate the role of these land to sea carbon and nutrient fluxes on the oceanic component and CO_2 exchange with the atmosphere during rapid flooding event. As an example, during this period of massive freshwater discharge between 15-14 ka resulting in the flooding of coastal areas, 18.4 GtC are transferred to the ocean carbon inventory (Figure 4), which is a significant fraction of the total input of 50.6 GtC resulting from flooding over the whole period (21-12 ka). Preliminary results also show that following this abrupt flooding event, local CO_2 outgassing of the ocean is occurring but is not enough to counterbalance the global ocean CO_2 uptake state.

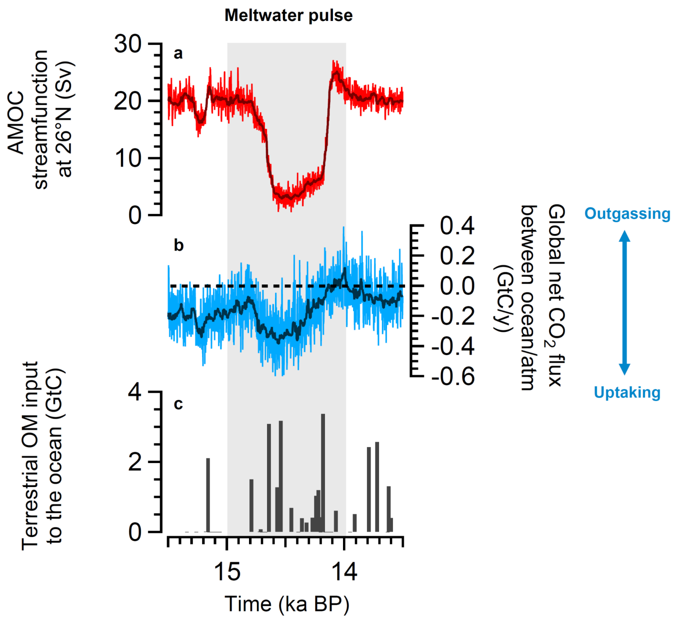

Figure 4: (a) Atlantic Meridional Overturning Circulation streamfunction at 26°N, (b) global net CO_2 flux between the ocean and the atmosphere and (c) total terrestrial organic matter input to the ocean (water column and sediment) during a large meltwater pulse of the last deglaciation.

Multiple sensitivity experiments have been planned for this year, focusing on time intervals within the last deglaciation that are marked by large meltwater inputs and then associated with large amounts of land-derived carbon and nutrients going into the ocean to investigate their role on the CO_2 variations. However, these simulations have not yet been performed. After 8 months without dedicated position on this topic and the consequences/delays related to the coronavirus, a recent position just started a few months ago to work on this. To date, only one sensitivity experiment is currently under progress during a 1000-years time-slice within the first meltwater pulse observed between 15-14 ka in the simulation.

WP CC.1-TP4 – Development of the PICO ice shelf cavity model into a “pop-up” model for use in transient glacial simulation
The current development can still be carried out with local computing resources. Therefore, no request for resources was made at the DKRZ.

4.2 CC2: Report on resources used in 2020

WP CC.2-TP1 – Data management
CC2 TP1 asked for 10TB /work for standardisation of model output Because of late start of the personnel the work started in late Summer and the resources were not used. For the next period CC2 TP1 created a dedicated project bm1192 for for holding the PalMod data pool.

WP CC.2-TP2 – Probabilistic model-data comparison of trends and shifts
There was no storage space used in 2020 so far. This is mainly because of delays in work due to the pandemic situation in 2020 as well as due to changes in chosen workflows.

WP CC.2-TP3 – The contribution of volcanic forcing to glacial climate variability
No specific request for resources was made at the DKRZ. We are still in an early development phase such that it was enough to use the shared resources of other CC.2 subprojects.

WP CC.2-TP4 – Development of a paleoclimate model and proxy comparison toolbox
There was no storage space used in 2020, mainly because of delays in work due to the pandemic situation in 2020.